Wu et al. *Zool. Res.* 2021, 42(3): 377−388
https://doi.org/10.24272/j.issn.2095-8137.2020.375

ZR | Zoological Research

Article Open Access

LIN28A inhibits *DUSP* family phosphatases and activates MAPK signaling pathway to maintain pluripotency in porcine induced pluripotent stem cells

Xiao-Long Wu[1,#], Zhen-Shuo Zhu[1,#], Xia Xiao[2,#], Zhe Zhou[1], Shuai Yu[1], Qiao-Yan Shen[1], Ju-Qing Zhang[1], Wei Yue[1], Rui Zhang[1], Xin He[1], Sha Peng[1], Shi-Qiang Zhang[1], Na Li[1,*], Ming-Zhi Liao[2,*], Jin-Lian Hua[1,*]

[1] *College of Veterinary Medicine*, *Shaanxi Centre of Stem Cells Engineering and Technology*, *Northwest A & F University*, *Yangling*, *Shaanxi* 712100, *China*

[2] *College of Life Science*, *Northwest A & F University*, *Yangling*, *Shaanxi* 712100, *China*

ABSTRACT

LIN28A, an RNA-binding protein, plays an important role in porcine induced pluripotent stem cells (piPSCs). However, the molecular mechanism underlying the function of *LIN28A* in the maintenance of pluripotency in piPSCs remains unclear. Here, we explored the function of *LIN28A* in piPSCs based on its overexpression and knockdown. We performed total RNA sequencing (RNA-seq) of piPSCs and detected the expression levels of relevant genes by quantitative real-time polymerase chain reaction (qRT-PCR), western blot analysis, and immunofluorescence staining. Results indicated that piPSC proliferation ability decreased following *LIN28A* knockdown. Furthermore, when *LIN28A* expression in the *sh*LIN28A2 group was lower (by 20%) than that in the negative control knockdown group (*sh*NC), the pluripotency of piPSCs disappeared and they differentiated into neuroectoderm cells. Results also showed that *LIN28A* overexpression inhibited the expression of *DUSP* (dual-specificity phosphatases) family phosphatases and activated the mitogen-activated protein kinase (MAPK) signaling pathway. Thus, *LIN28A* appears to activate the MAPK signaling pathway to maintain the pluripotency and proliferation ability of piPSCs. Our study provides a new resource for exploring the functions of *LIN28A* in piPSCs.

Keywords: LIN28A; MAPK; Pluripotency; piPSCs; DUSP

INTRODUCTION

LIN28A has two nucleic acid-binding domains: i.e., cold shock domain and zinc-knuckle domain (Moss et al., 1997), which bind specific sequences and play vital roles in physiology (Balzer et al., 2010; Hafner et al., 2013; Polesskaya et al., 2007; Shyh-Chang & Daley, 2013; Xu et al., 2009; Zhu et al., 2011). In addition to RNA binding, LIN28A also functions as a transcription factor during reprogramming (Liao et al., 2008;

Received: 16 February 2021; Accepted: 14 May 2021; Online: 17 May 2021

Foundation items: This work was supported by the National Key Research, Development Program of China-Stem Cell and Translational Research (2016YFA0100200), National Natural Science Foundation of China (32072806, 31572399, 61772431, 62072377), Program of Shaanxi Province Science and Technology Innovation Team (2019TD-036), Fundamental Research Funds for the Central Universities, Northwest A & F University (Z1090219146, Z102022004)

[#]Authors contributed equally to this work

*Corresponding authors, E-mail: lina2017@nwafu.edu.cn; liaomz@nwsuaf.edu.cn; jinlianhua@nwsuaf.edu.cn

Yu et al., 2007). *LIN28A* can regulate the naïve to primed state conversion by regulating stem cell metabolism in induced pluripotent stem cells (iPSCs) (Zhang et al., 2016). Knockdown of *LIN28A* promotes the transformation of embryonic stem cells (ESCs) into the naïve state (Chandrasekaran et al., 2017; Kumar et al., 2014; Marks et al., 2012), and *LIN28A* regulates pluripotent state transformation in mouse ESCs by inhibiting *DPPA3* expression (Sang et al., 2019). However, few studies have explored *LIN28A* in porcine iPSCs (piPSCs) and the mechanism underlying *LIN28A* functions in piPSCs remains unclear. Previous research has indicated that inhibiting *LIN28A* expression via miR-370 may reduce piPSC proliferation ability and alkaline phosphatase (AP) activity, and up-regulate the expression of differentiation-relevant genes (Zhang et al., 2017). This finding differs from studies on *LIN28A* in human and mouse PSCs (Zhang et al., 2017). Thus, *LIN28A* may play a different role in piPSCs.

The mitogen-activated protein kinase (MAPK) signaling pathway plays important roles in controlling cell cycle, differentiation, proliferation, and apoptosis (Pearson et al., 2001; Shaul & Seger, 2007). Activation of the mitogen-activated protein kinase kinase (MEK)/extracellular signal-regulated kinase (ERK) signaling pathway can promote the differentiation of mouse ESCs (mESCs), while its suppression can prevent mESC differentiation (Burdon et al., 1999; Deathridge et al., 2019). MESCs can be cultured in the 2i (CHIR99021 and PD0325901) system using MEK1 and glycogen synthase kinase-3 (GSK3) inhibitors (Ying et al., 2008). *In vitro* activation of MAPK signaling helps maintain the primed state, whereas repression of MAPK signaling through ERK inhibition reverts PSCs to the naïve state (Chen et al., 2015; Hackett & Surani, 2014; Kalkan et al., 2019; Ying et al., 2008). The dual-specificity phosphatase (DUSP) family dephosphorylates MAPK signaling and plays an important role in regulating the duration, magnitude, and spatiotemporal profiles of MAPK activity (Caunt & Keyse, 2013; Chen et al., 2019). According to previous reports, the pluripotency of piPSCs is rapidly lost following treatment with 1.0 μmol/L MEK1 inhibitor PD0325901 (Gao et al., 2019). Thus, piPSCs may differ from mESCs in MEK/ERK signaling requirements and inhibiting MAPK may impair their pluripotency.

Our laboratory previously reported that the doxycycline (DOX)-inducible porcine PSC line (DOX-piPSC) can be cultured with cytokines (leukemia inhibitory factor (LIF), basic fibroblast growth factor (bFGF)), signaling inhibitors (CHIR099021, SB431542), feeder cells, and serum (Ma et al., 2018; Zhu et al., 2021). PiPSCs can be maintained in the pluripotent state with the addition of DOX, but differentiate after its withdrawal (Ma et al., 2018; Zhang et al., 2017; Zhu et al., 2021). In this study, we explored the function of *LIN28A* by knockdown and overexpression. Results showed that proliferation ability and colony size decreased significantly when *LIN28A* was knocked down. Furthermore, piPSCs overexpressing *LIN28A* maintained colonies after DOX withdrawal. We also performed total RNA sequencing (RNA-seq) of negative control knockdown in the OEOCT4-piPSC group (OEOCT4-*sh*NC) and *LIN28A* knockdown in the OEOCT4-piPSC group (OEOCT4-*sh*LIN28A2) after withdrawal of DOX. Based on RNA-seq analysis, a reduction in *LIN28A* expression up-regulated differentiation-relevant gene expression and promoted neuroectoderm differentiation. *LIN28A* also inhibited the expression of *DUSP* family members and activated the MAPK signaling pathway to maintain the pluripotency of piPSCs.

MATERIALS AND METHODS

Cell culture

HEK293T cells were cultured in 6-well plates (140675, Thermo Fisher Scientific, USA) using Dulbecco's Modified Eagles Medium (DMEM) (Hyclone, USA) with 10% fetal bovine serum (FBS) (VIS, New Zealand). Mouse embryonic fibroblasts (MEFs) were cultured in 100 mm vessels (140675, Thermo Fisher Scientific, USA) using DMEM (10% FBS) and treated with mitomycin for 2.5 h. The mitomycin-treated MEFs were then passaged at 1×10^5 cells/well into 12-well plates (140675, Thermo Fisher Scientific, USA) as the culture matrix for piPSCs. DOX-piPSCs were cultured in the LB2i system, which included 15% FBS, 0.1 mmol/L nonessential amino acids (NEAA) (Gibco, USA), 1 mmol/L L-glutamine (Gibco, USA), 10 ng/mL LIF (14890-HNAE, Sino Biological, China), 10 ng/mL bFGF (10014-HNAE, Sino Biological, China), 0.1 mmol/L β-mercaptoethanol (M3148, Sigma-Aldrich, USA), 3 μmol/L CHIR99021 (HY-10182, MCE, USA), 2 μmol/L SB431542 (S1067, Selleck, USA), and 4 μg/mL DOX (D9891, Sigma-Aldrich, USA). The piPSCs were passaged using TrypLE™ Select (Invitrogen, USA) into single cells at 2×10^4 cells/well in a 12-well plate every 5–6 days (Ma et al., 2018).

Cell growth curve

To obtain the cell growth curves for the negative control knockdown group (*sh*NC), *LIN28A* knockdown group (*sh*LIN28A1/2), negative control overexpression group (OENC), and *LIN28A*-overexpression group (OELIN28A), cells were cultured in 24-well plates at an initial density of 1×10^4 cells/well. The piPSCs of the *sh*NC, *sh*LIN28A1/2, OENC, and OELIN28A groups were cultured in the LB2i system for 5 days and cell number in each group was counted daily using a blood counting chamber.

Vector construction and cloning

All lentivirus backbone vectors were derived from pCDH-CMV-MCS-EF1-GreenPuro using a Seamless Cloning and Assembly Kit (Novoprotein, China).

Construction of short hairpin RNA (*sh*RNA) vector

Here, *sh*RNA of porcine LIN28A was designed using BLOCK-iT™ RNAi Designer (https://rnaidesigner.thermofisher.com/rnaiexpress/design.do) (Supplementary Table S1) and the interference fragments were synthesized (enzymatic cleavage sites were BamHI and EcoRI). The double-stranded fragment was then connected to pCDH-U6-MCS-EF1-GFP-T2A-PURO linearized by BamHI and EcoRI via the T4 DNA ligase. All interference vectors were transfected into DOX-piPSCs and their interference efficiencies were verified, i.e., 80.78% (*sh*LIN28A1) and 85.14% (*sh*LIN28A2).

Construction of overexpression vector

Porcine testis cDNA was used as a template, and the porcine LIN28A fragment was successfully obtained using Prime Star Max DNA Polymerase (R045B, Takara, Japan). The fragment was then connected to pCDH-EF1-MCS-T2A-PURO linearized by BamHI and EcoRI via the T4 DNA ligase. The overexpression vector of porcine LIN28A was transduced to DOX-piPSCs and overexpression efficiency was detected.

Lentiviral packaging

HEK293T cells were cultured in a 6-well plate (140675, Thermo Fisher Scientific, USA) at a density of 80%–90%. Lentiviral plasmids and packaged viral vectors (pVSV-G and psPAX2) were transfected into the HEK293T cells using polyethyleneimine (PEI, Sigma-Aldrich, USA). In total, 1 μg of pVSV-G, 1 μg of psPAX2, and 2 μg of the lentiviral vectors were mixed in 12 μL of PEI (1 mg/mL). The plasmid mixture was then rested for 15 min at room temperature, after which 200 μL of optiMEM was added. After 12 h, the culture medium was replaced with DMEM. The HEK293T cells were then cultured for 48–72 h to produce lentiviral particles. The lentiviral particles (culture supernatant) were gathered and filtered through a 0.45 μm filter to remove cell debris.

Lentiviral particle transduction

The piPSCs were cultured in a 12-well plate covered with MEF at 37 °C for 12 h. The lentiviral particles (supernatant) and piPSC medium were mixed at a 1:1 ratio and 4 μg/mL polybrene was added to the mixture. The piPSCs were cultured with mixed medium at 37 °C for 8–12 h, which was then replaced by new iPSC medium. Fluorescence was observed after 2–3 days and puromycin was used to select puro-positive cells after the piPSCs were cultured for 1 week.

Total RNA extraction, reverse-transcription polymerase chain reaction (PCR), and quantitative real-time PCR (qRT-PCR)

Total RNA was extracted using the RNAiso Plus reagent (9108, Takara, Japan) via the guanidine isothiocyanate phenol-chloroform method (Chomczynski & Sacchi, 2006). Extracted RNA quality was detected using a NanoDrop™ spectrophotometer (Thermo Fisher Scientific, USA) and agarose gel electrophoresis. Then, 2 μg of RNA was reverse transcribed to obtain cDNA using a FastKing RT Kit (with gDNase) (KR116, day root). Quantitative RT-PCR was performed using a SuperReal PreMix Plus (SYBR Green) (FP215, Tiangen, China) via a three-step process. The primers used for qRT-PCR are shown in Supplementary Table S2.

Western blot analysis

The piPSCs cultured for 5 days were digested by TrypLE™ Select (Invitrogen, USA), and the same volume of DMEM+ was added to neutralize the reaction. The mixture was then transferred to a 1.5 mL tube and centrifuged at 5 000 *g* at 4 °C for 3 min. The supernatant of the culture medium was discarded and RIPA lysate (P0013B, Beyotime, China) with 10 mmol/L protease inhibitor PMSF (Sigma-Aldrich, USA) and phosphatase inhibitor was used to lyse the piPSCs for 30 min. Then, 5×SDS-PAGE loading buffer (JC-PE007, GENSHARE G, China) was added, followed by heating at 100 °C for 5 min. The protein samples were added to 8%–12% SDS-PAGE gel and run at 100 V for 1.5 h, then transferred onto polyvinylidenefluoride (PVDF) membranes at 15 V for 45 min using a Trans-Blot SD Semi-Dry Electrophoretic Transfer Cell (BioRad, USA). The membranes were then blocked using 8% skim milk (5% bovine serum albumin (BSA) in phospho-p44/42 MAPK and p44/42 MAPK) at room temperature for 2 h. Primary antibodies, including LIN28A (1 : 400; Santa Cruz Biotechnology, USA), proliferating cell nuclear antigen (PCNA) (1 : 500; Boster, China), FLAG (1 : 1 000; Sigma-Aldrich, USA), β-actin (1 : 4 000; Sungene Biotech, China), phospho-p44/42 MAPK (1 : 1 000; Cell Signaling Technology, USA), and p44/42 MAPK (1 : 1 000; Cell Signaling Technology, USA), were diluted in TBS-T buffer (20 mmol/L Tris HCl/pH 8.0, 150 mmol/L NaCl, 0.05% Tween 20) according to the instructions and then incubated at 4 °C for 12 h.

The PVDF membranes were washed using TBS-T buffer at room temperature for 15 min. AffiniPure Goat Anti-Mouse/Rabbit IgG (H+L) was then used to combine the antibody at 37 °C for 1 h (Hu et al., 2020). The membranes were washed using TBS-T buffer at room temperature for 15 min and a Tanon-5200 automatic chemiluminescence image analysis system (Tanon, China) was used to detect the horseradish peroxidase (HRP) signal. The relative grays of the western blots were analyzed by ImageJ.

Immunofluorescent staining

After twice washing with PBS, the piPSCs (cultured for 5 days) were fixed in 4% paraformaldehyde (pH 7.4) at room temperature for 15 min. We used 0.1% Triton-100 to perforate the membranes at room temperature for 10 min. Then, 10% FBS was used to block the membranes at room temperature for 1 h. The membranes were incubated with primary antibodies, including LIN28A (1 : 200; Santa Cruz Biotechnology, USA) and FLAG (1 : 1 000; Sigma-Aldrich, USA), for 12 h at 4 °C and then washed three times with PBS. The membranes were then incubated with goat anti-mouse IgG (H+L) secondary antibody Alexa Fluor 488 conjugate (1 : 500; ZSGB-BIO, China) at room temperature for 1 h and nuclei were stained with Hoechst33342 (1 : 1 000) at room temperature for 5 min (Ma et al., 2019; Wei et al., 2021).

AP staining

The piPSCs (cultured for 5 days) were fixed in 4% paraformaldehyde (pH 7.4) at room temperature for 15 min, with AST Fast Red TR and α-naphthol AS MX phosphate (Sigma-Aldrich, USA) then used to stain the cells according to the manufacturer's instructions. The piPSCs were incubated in 1.0 mg/mL Fast Red TR, 0.4 mg/mL α-naphthol AS-MX, and 0.1 mmol/L Tris-HCL 8.8 buffer at room temperature for 20 min. The AP-positive piPSCs clones showed red (Zhang et al., 2017). Images were obtained using a Nikon phase difference microscope.

5-Ethynyl-2'-deoxyuridine (EdU) staining

EdU detection was performed on 3 d cultured piPSCs according to the Cell-Light EdU Apollo567 *In-Vitro* Kit instructions (RiboBio, China). The PiPSCs were exposed to 50 μmol/L EdU medium at 37 °C for 20 min, and then fixed in

4% paraformaldehyde (pH 7.4) at 37 °C for 15 min. After this, 2 mg/mL glycine was added to neutralize excess aldehyde. The piPSCs were then exposed to 1×Apollo staining solution at 37 °C for 30 min and washed three times with PBS. We then used 0.1% Triton-100 to perforate the membranes for 10 min at 37 °C and the nuclei were stained with Hoechst33342 (1 : 1 000).

RNA-seq

To explore the molecular mechanism of LIN28A in piPSCs, the *sh*NC and *sh*LIN28A2 groups with two biological replicates underwent RNA-seq. Total RNA was extracted using RNAiso Plus reagent (9108, Takara, Japan) with the guanidine isothiocyanate phenol-chloroform method (Chomczynski & Sacchi, 2006). Extracted RNA quality was detected using a NanoDrop™ spectrophotometer (Thermo Fisher Scientific, USA) and agarose gel electrophoresis. Total RNA was treated using Oligo dT-enriched mRNA and purification. Fragmented RNA was then reverse-transcribed using random N6 primers to form double-stranded DNA (second-strand cDNA synthesis with dUTP instead of dTTP). Next, 3'adenylated and adaptor ligation was added to the end of the synthesized double-stranded DNA, which was amplified using PCR with specific primers. The PCR products were thermally denatured into a single strand and a bridging primer was used to form a loop to obtain a single-stranded circular DNA library. Quality control (QC) was conducted on the DNA library, and sequencing was then performed on the DNBSEQ platform. Raw reads were filtered through QC using SOAPnuke. Finally, Bowtie2 was used to align the clean reads. Heatmaps were plotted through pheatmap (v1.0.12) to represent specific gene expression levels. Both Gene Ontology (GO) and Kyoto Encyclopedia of Genes and Genomes (KEGG) pathway analyses were conducted using clusterProfiler (v3.12.0). An adjusted *P*-value of <0.05 and Q-value of <0.05 were used to define the working threshold for statistical significance.

Statistical analysis

Two-tailed *t*-tests were used to determine significant differences between two groups and one-way or two-way analysis of variance (ANOVA) was used to determine significant differences between three groups. All data are shown as mean±standard error of the mean (*SEM*). Differences were considered significant when $P<0.05$.

RESULTS

Effects of *LIN28A* on piPSC proliferation ability

LIN28A mRNA expression fluctuated under different concentrations of DOX (Supplementary Figure S1A), reaching a maximum level with the addition of 2 μg/mL DOX and then gradually decreasing with increasing concentrations of DOX (4 μg/mL to 16 μg/mL). Interestingly, colony size decreased with *LIN28A* expression after the administration of increasing concentrations of DOX (4 μg/mL to 16 μg/mL) (Supplementary Figure S1B).

Therefore, we next explored the relationship between the expression level of *LIN28A* and colony size. We designed two pairs of *sh*RNA and constructed a *LIN28A* interference vector. The interference efficiency of the vector was detected by qRT-PCR. Results showed that the mRNA and protein expression levels of *LIN28A* decreased significantly in the *sh*LIN28A1/2 groups (Figure 1A, B). Compared with the *sh*NC group, colony size and AP activity decreased following *LIN28A* knockdown (Figure 1C). The cell growth curve showed that proliferation ability and protein expression of proliferating cell nuclear antigen (PCNA) decreased significantly when *LIN28A* was knocked down (Figure 1B, D). These results indicate that the proliferation ability of piPSCs decreased after *LIN28A* knockdown.

To further explore its function, porcine *LIN28A* was overexpressed in piPSCs (OELIN28A group) and its expression level was detected by qRT-PCR, western blotting, and immunofluorescent staining (Supplementary Figure S2A, B). Compared to the negative control overexpression group with DOX (OENC+DOX+), colony size and AP activity in the OELIN28A+DOX+ group did not change significantly (Supplementary Figure S2C). Furthermore, compared to the OENC+DOX+ group, the percentage of EdU-positive cells in the OELIN28A+DOX+ group did not change significantly (Supplementary Figure S2D, E). The cell growth curve also showed that there was no significant change in proliferation ability after overexpression of *LIN28A* (Figure 1D).

The DOX-piPSCs were maintained in the pluripotent state with DOX but differentiated after its withdrawal (Figure 1E, first column), consistent with previous studies (Ma et al., 2018; Zhang et al., 2017). The colonies in the negative control overexpression group without DOX (OENC+DOX−) gradually disappeared (Figure 1E, first column). However, colonies in the OELIN28A group without DOX (OELIN28A+DOX−) were still observed, although their size and number decreased significantly compared with the OENC+DOX+ and OELIN28A+DOX+ groups (Figure 1E, F). These findings indicate that LIN28A can maintain typical colonies after withdrawal of DOX. Pluripotent-relevant genes were detected by qRT-PCR. Results showed that the expression levels of *SALL4* and *NANOG* increased and decreased, respectively, in the OELIN28A groups (Figure 1G). Thus, the knockdown and overexpression experiments showed that *LIN28A* plays a vital role in maintaining the proliferation ability of piPSCs.

Effects of *LIN28A* on piPSC pluripotency

LIN28A mRNA expression levels in the piPSCs fluctuated with DOX concentrations (Supplementary Figure S1A). Therefore, we explored the function of *LIN28A* after excluding the influence of DOX. Results showed that OEOCT4-piPSCs maintained colonies and proliferation ability in the absence of DOX (Supplementary Figure S3A). Therefore, experiments were performed on piPSCs overexpressing *OCT4* (OEOCT4-piPSCs).

The interference efficiency of *sh*LIN28A1 and *sh*LIN28A2 was similar, but the proliferation rate of *sh*LIN28A2 decreased more obviously according to the cell growth curve and expression of PCNA, so subsequent experiments were performed on the *sh*LIN28A2 groups. Compared with the OEOCT4-*sh*NC group without DOX, colony size decreased in the OEOCT4-*sh*LIN28A2 group without DOX (Figure 2A, B), consistent with the *sh*LIN28A2 group results (Figure 1C). The

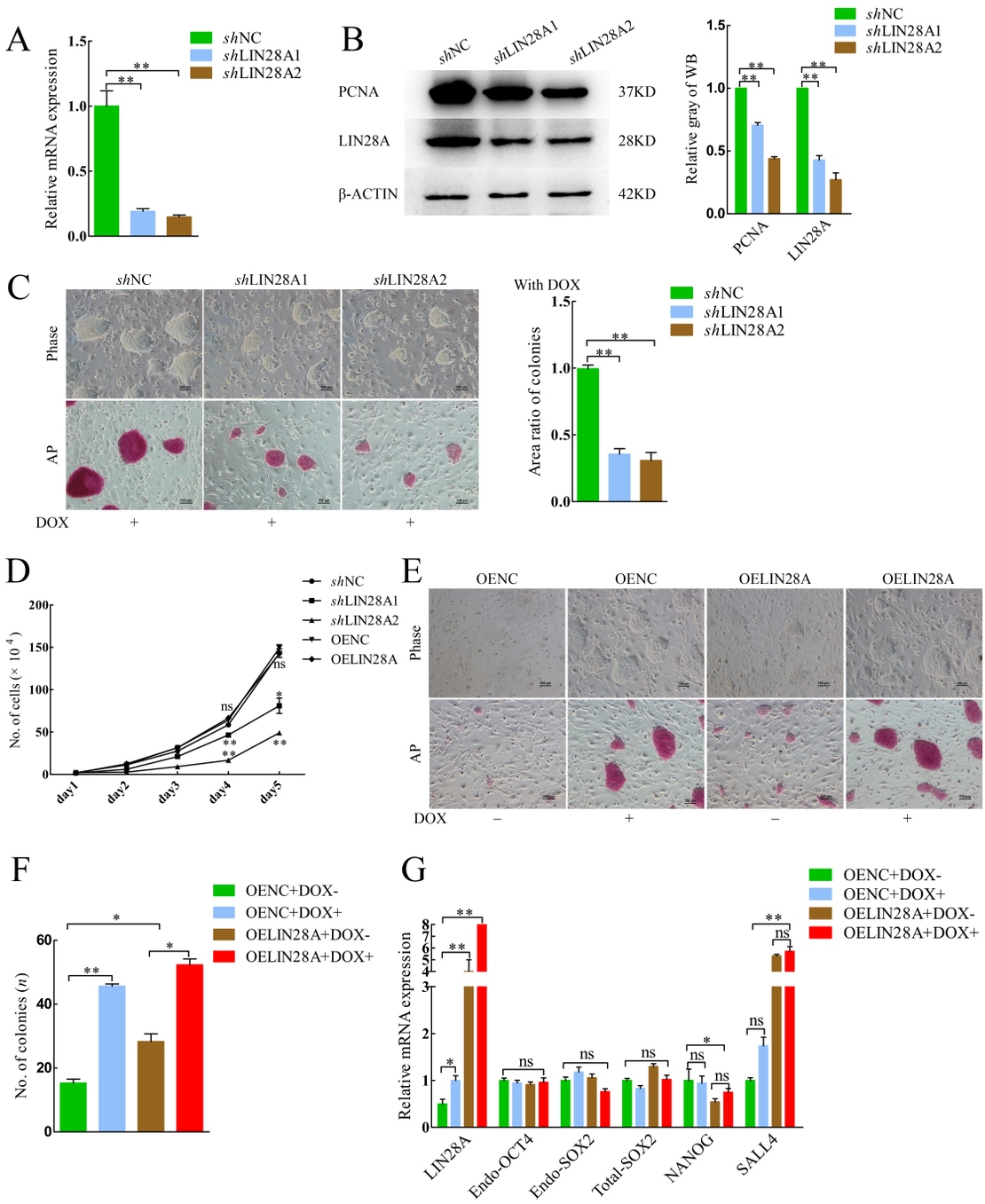

Figure 1 Effects of *LIN28A* on piPSC proliferation ability

A: *LIN28A* mRNA expression levels in *sh*NC, *sh*LIN28A1, and *sh*LIN28A2 groups with DOX were detected by qRT-PCR. Data are mean±*SEM*. **: *P*<0.01. *n*=3. B: Left: PCNA and LIN28A protein expression levels in *sh*NC, *sh*LIN28A1, and s*h*LIN28A2 groups with DOX were detected by western blotting. Data are mean±*SEM*. *n*=2. Right: Quantitative analysis of PCNA and LIN28A protein expression levels in *sh*NC, *sh*LIN28A1, and *sh*LIN28A2 groups with DOX is shown in histogram. Data are mean±*SEM*. **: *P*<0.01. *n*=3. C: Left: Morphology and AP staining of *sh*NC, *sh*LIN28A1, and *sh*LIN28A2 groups with DOX. Scale bar: 100 μm for phase and 100 μm for AP. Right: Area ratio of colonies in *sh*NC, *sh*LIN28A1, and *sh*LIN28A2 groups with DOX. **: *P*<0.01. D: Growth curve in *sh*NC, *sh*LIN28A1, *sh*LIN28A2, OENC, and OELIN28A groups with DOX. Data are mean±*SEM*, *: *P*<0.05, **: *P*<0.01. *n*=3. E: Morphology and AP staining of the negative control overexpression group without DOX (OENC+DOX−), negative control overexpression group with DOX (OENC+DOX+), OELIN28A group without DOX (OELIN28A+DOX−), and OELIN28A group with DOX (OELIN28A+DOX+). Scale bar: 100 μm. F: Number of colonies in OENC+DOX−, OENC+DOX+, OELIN28A+DOX−, and OELIN28A+DOX+ groups. Data are mean±*SEM*. *: *P*<0.05, **: *P*<0.01. G: mRNA expression levels of pluripotent genes in OENC+DOX−, OENC+DOX+, OELIN28A+DOX−, and OELIN28A+DOX+ groups were detected by qRT-PCR. Data are mean±*SEM*. *: *P*<0.05, **: *P*<0.01. *n*=3. ns: No significance.

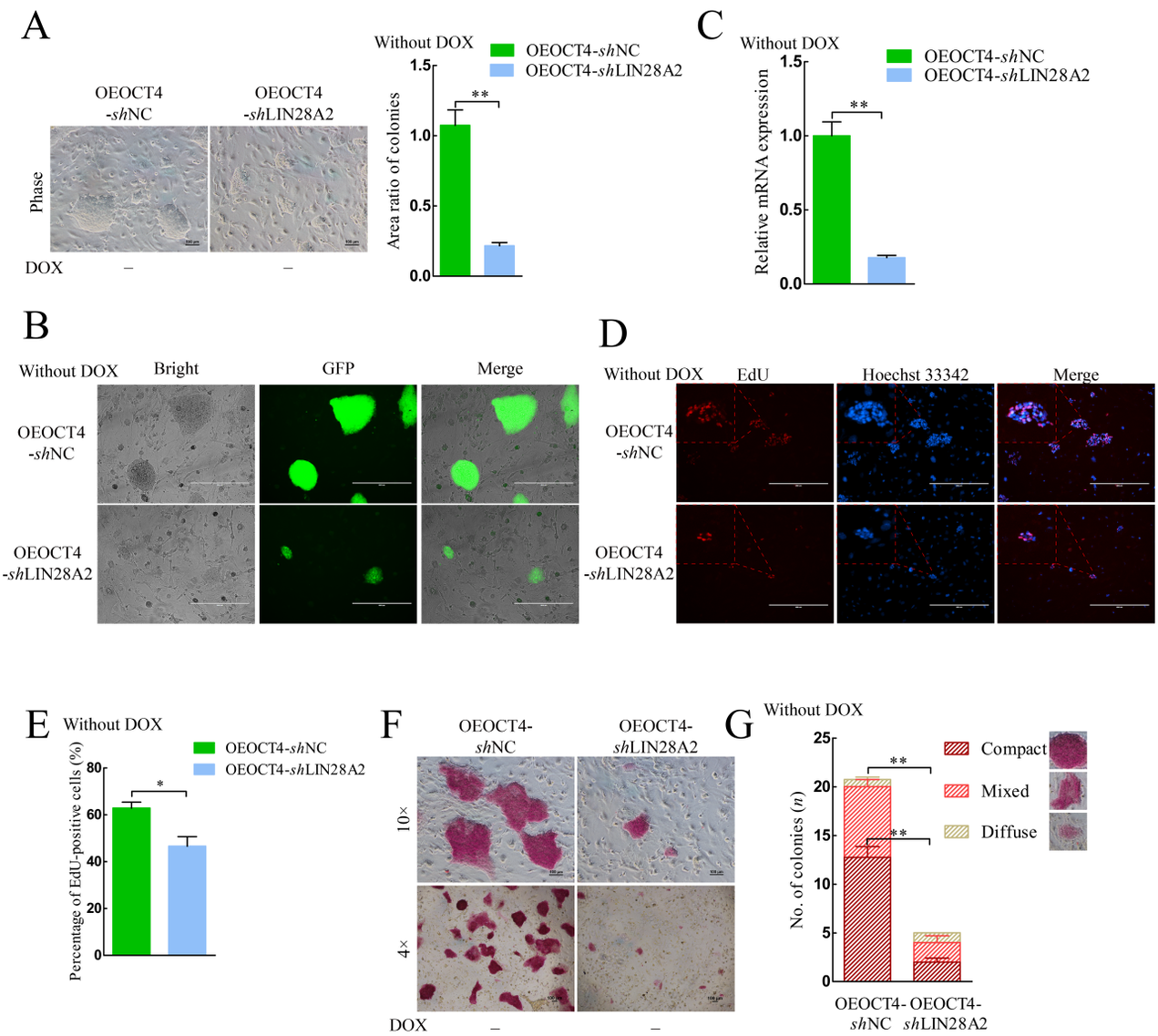

Figure 2 Effects of *LIN28A* on piPSC pluripotency

A: Left: Morphology of OEOCT4-*sh*NC and OEOCT4-*sh*LIN28A2 groups without DOX. Scale bar: 100 μm. Right: Area ratio of colonies in OEOCT4-*sh*NC and OEOCT4-*sh*LIN28A2 groups without DOX. **: $P<0.01$. B: Morphology of OEOCT4-*sh*NC and OEOCT4-*sh*LIN28A2 groups without DOX using fluorescence microscopy. Scale bar: 400 μm. C: LIN28A mRNA expression levels in OEOCT4-*sh*NC and OEOCT4-*sh*LIN28A2 groups without DOX were detected by qRT-PCR. Data are mean±*SEM*. *: $P<0.05$, **: $P<0.01$. $n=3$. D: EdU staining of OEOCT4-*sh*NC and OEOCT4-*sh*LIN28A2 groups cultured on third day without DOX. Scale bar: 400 μm. E: Percentage of EdU-positive cells in OEOCT4-*sh*NC and OEOCT4-*sh*LIN28A2 groups cultured on third day without DOX. Scale bar: 400 μm. Data are mean±*SEM*. *: $P<0.05$. $n=3$. F: AP staining of OEOCT4-*sh*NC and OEOCT4-*sh*LIN28A2 groups without DOX. Scale bar: 100 μm for AP. G: Quantification of AP-positive colonies in OEOCT4-*sh*NC and OEOCT4-*sh*LIN28A2 groups without DOX. Data are mean±*SEM*. *: $P<0.05$, **: $P<0.01$. $n=3$.

LIN28A mRNA expression level was detected again and was significantly decreased (Figure 2C). The percentage of EdU-positive cells also decreased significantly in the OEOCT4-*sh*LIN28A2 group (Figure 2D, E). The AP staining assays showed that AP activity and colony size decreased significantly in the OEOCT4-*sh*LIN28A2 group without DOX (Figure 2F). Based on AP staining assays (Sang et al., 2019), colonies can be classified into three shapes: i.e., typical primed diffuse-shape, compact dome-shape, and mixed-shape. Compact dome-shaped colonies in the OEOCT4-*sh*NC group accounted for 60% of total colonies in this group, while compact dome-shaped colonies in the OEOCT4-*sh*LIN28A2 group accounted for ~50%; however, the total number of colonies in the OEOCT4-*sh*LIN28A2 group decreased significantly and colonies in the OEOCT4-*sh*LIN28A2 group basically disappeared (Figure 2G).

The results obtained for the OEOCT4-*sh*LIN28A2 group with DOX were similar to that of the OEOCT4-*sh*LIN28A2

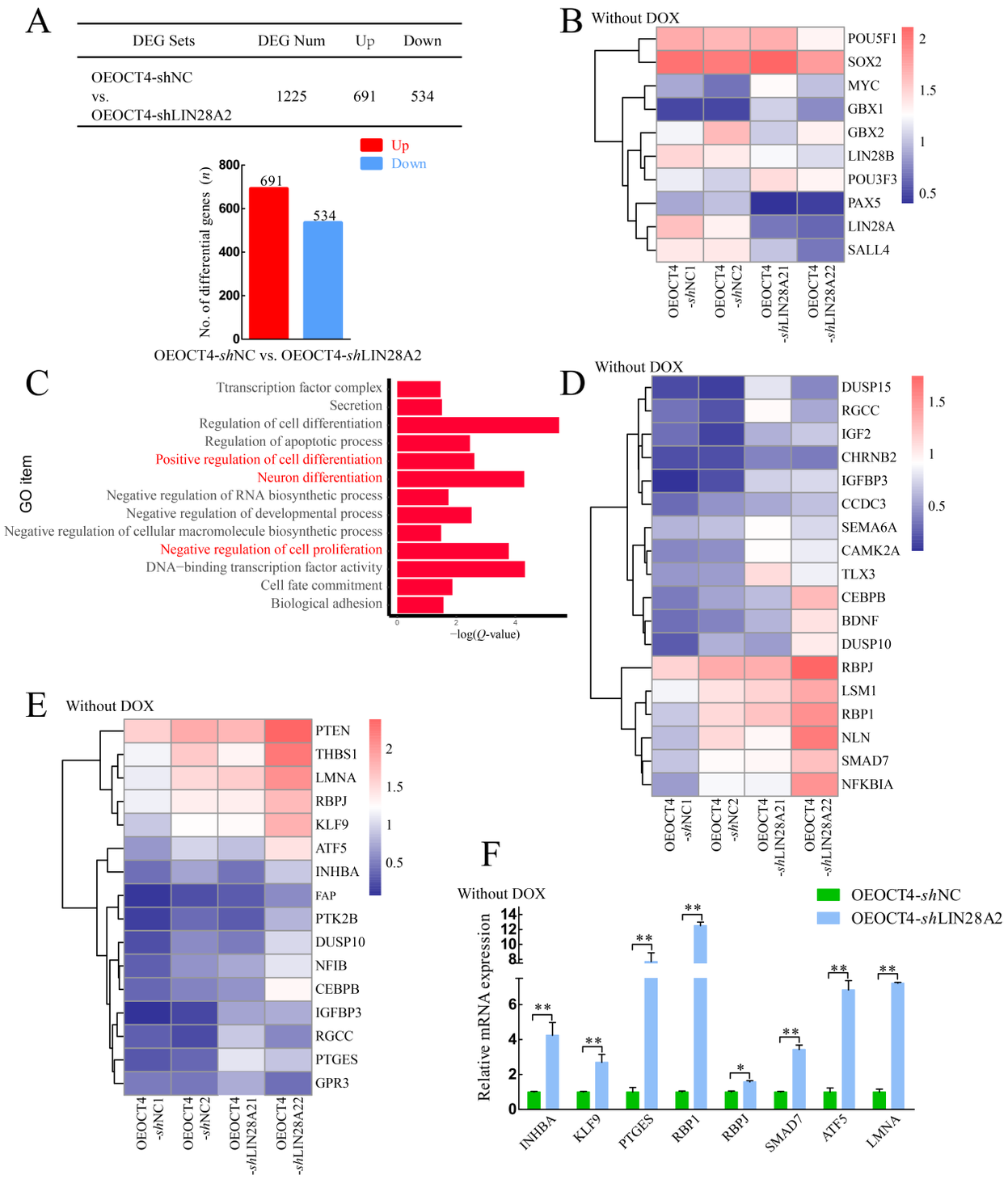

Figure 3 *LIN28A* inhibited expression of differentiation-related genes

A: Number of up- and down-regulated DEGs in OEOCT4-*sh*NC and OEOCT4-*sh*LIN28A2 groups without DOX. B: Heat map shows expression of pluripotent genes in OEOCT4-*sh*NC and OEOCT4-*sh*LIN28A2 groups without DOX based on RNA-seq. C: Gene Ontology enrichment analysis of up-regulated DEGs, highlighting positive regulation of cell differentiation, neuronal differentiation, and negative regulation of cell proliferation. D: Heat map showing expression of genes involved in negative regulation of cell proliferation based on RNA-seq. E: Heat map showing expression of genes involved in positive regulation of cell differentiation and neuronal differentiation based on RNA-seq. F: mRNA expression levels of genes involved in positive regulation of cell differentiation, neuronal differentiation, and negative regulation of cell proliferation were detected by qRT-PCR. Data are mean±*SEM*. *: $P<0.05$, **: $P<0.01$. $n=3$.

group without DOX. Compared to the OEOCT4-*sh*NC group with DOX, colony size (Supplementary Figure S3B, E) and AP activity in the OEOCT4-*sh*LIN28A2 group with DOX decreased significantly (Supplementary Figure S3E). The percentage of EdU-positive cells also decreased significantly in the OEOCT4-*sh*LIN28A2 group with DOX (Supplementary Figure S3C, D). The number of compact dome-shaped colonies in the OEOCT4-*sh*LIN28A2 group with DOX decreased significantly compared with that in the OEOCT4-*sh*NC group (Supplementary Figure S3F). These results indicate that pluripotency decreased after *LIN28A* knockdown and *LIN28A* plays a vital role in maintaining the pluripotency of piPSCs.

LIN28A inhibited expression of differentiation-related genes

We performed total RNA-seq on two samples in the OEOCT4-*sh*NC and OEOCT4-*sh*LIN28A2 groups after withdrawal of DOX. The table in Figure 3A shows the number of up- and down-regulated differentially expressed genes (DEGs) in the OEOCT4-*sh*NC and OEOCT4-*sh*LIN28A2 groups after DOX withdrawal. Among them, the expression levels of *OCT4*/*SOX2*/*LIN28B* showed no significant changes, but the expression level of *LIN28A* decreased in the OEOCT4-*sh*LIN28A2 group (Figure 3B). After analyzing the RNA-seq results, GO analysis showed enrichment in positive regulation of cell differentiation, neuronal differentiation, negative regulation of cell proliferation, and DNA-binding transcription factor activity (Figure 3C). The expression of genes involved in the negative regulation of cell proliferation increased significantly in the OEOCT4-*sh*LIN28A2 group based on heat map and qRT-PCR (Figure 3D, F), which may explain the decline in piPSC proliferation ability following *LIN28A* knockdown. In addition, the heat map and qRT-PCR results showed that the expression levels of genes involved in neuronal differentiation and positive regulation of cell differentiation also increased significantly in the OEOCT4-*sh*LIN28A2 group (Figure 3D, F), which may explain the significant decrease in AP activity after *LIN28A* knockdown. These data indicate that *LIN28A* can inhibit the expression of differentiation-related genes in piPSCs and maintain the proliferation ability and pluripotency of piPSCs.

LIN28A inhibited expression of *DUSP* family and activated MAPK signaling pathway

Based on KEGG analysis, the primary enriched pathways included Axon guidance, Notch signaling pathway, and MAPK signaling pathway (Figure 4A). The MAPK signaling pathway plays an important role in pigs, and its inhibition can result in loss of pluripotency in porcine PSCs (Gao et al., 2019). Both heat map and qRT-PCR analyses showed that the mRNA expression levels of *DUSP*-family members increased in the OEOCT4-*sh*LIN28A2 group (Figure 4B, C), and the protein expression levels of ERK and phospho-ERK (p-ERK) in the OEOCT4-*sh*LIN28A2 group significantly increased and decreased, respectively (Figure 4D). These findings indicate that the MAPK signaling pathway is inactivated following LIN28A knockdown.

The *DUSP* mRNA expression levels were significantly decreased (Figure 4E) and the ERK and p-ERK protein expression levels were significantly decreased and increased, respectively, when *LIN28A* was overexpressed (Figure 4F). These results indicate that the MAPK signaling pathway was activated when *LIN28A* was overexpressed and *LIN28A* activated the MAPK signaling pathway by inhibiting the *DUSP*-family phosphatases. Results showed that cell proliferation ability and AP activity decreased when the MEK1 inhibitor (PD0325901) was used, consistent with the phenomena in the OEOCT4-*sh*LIN28A2 cells (Figure 4G). Cell proliferation ability and AP activity decreased with the addition of 1 μmol/L PD0325901, but this decrease was rescued by the overexpression of *LIN28A* (Figure 4H). These results suggest that *LIN28A* can maintain the pluripotency and proliferation ability of piPSCs by activating the MAPK signaling pathway.

DISCUSSION

PiPSCs can be generated using human OCT4, SOX2, KLF4, and c-MYC lentiviruses in porcine fetal fibroblasts (Esteban et al., 2009; Ezashi et al., 2009). All piPSCs can exhibit terminal differentiation and generation of teratoma *in vivo*, but none can produce chimeric offspring and germline transmission, suggesting that their pluripotency may be defective (Cheng et al., 2012; Esteban et al., 2009; Ezashi et al., 2009; Xue et al., 2016; Zhang et al., 2015, 2017). In the past several years, various laboratories have obtained piPSCs and modified the culture system (Cheng et al., 2012; Haraguchi et al., 2012; Hou et al., 2016; Xu et al., 2020; Xue et al., 2016; Zhang et al., 2015, 2017). Here, we attempted to obtain naïve piPSCs by modifying the patterns of gene expression.

Lin28a is the on-off switch between naïve and primed states. PSCs convert to the naïve state when *Lin28a* decreases, but to the primed state when *Lin28a* increases (Marks et al., 2012). Interestingly, in our study, piPSC proliferation, colony size, and AP activity all decreased following *LIN28A* knockdown (Figure 1B–D). We also found that the LIN28A mRNA expression level in piPSCs fluctuated with DOX concentration as LIN28A is regulated by OCT4/SOX2 (Supplementary Figure S1A) (Buganim et al., 2012). Therefore, we further explored the function of LIN28A excluding the influence of DOX. Results showed that the DOX-piPSCs started to differentiate after the withdrawal of DOX (Figure 1E, first column). By exploring single pluripotency gene function using a lentiviral overexpression system, we found that piPSCs maintained typical colonies after withdrawal of DOX when OCT4 was overexpressed (Supplementary Figure S3A) (Zhu et al., 2021). Compared with piPSCs, the cell proliferation and AP activities of the OEOCT4-piPSCs after DOX withdrawal showed no obvious differences. Therefore, experiments were performed on OEOCT4-piPSCs, with similar results as for piPSCs. Based on RNA-seq, we demonstrated that the pluripotency of the piPSCs disappeared and piPSCs differentiated into neuroectoderm cells when *LIN28A* was knocked down. *Lin28a* is also highly expressed in ESCs and is downregulated in response to differentiation (Balzer et al., 2010; Richards et al., 2004; Yang & Moss, 2003). Moreover, the expression levels of

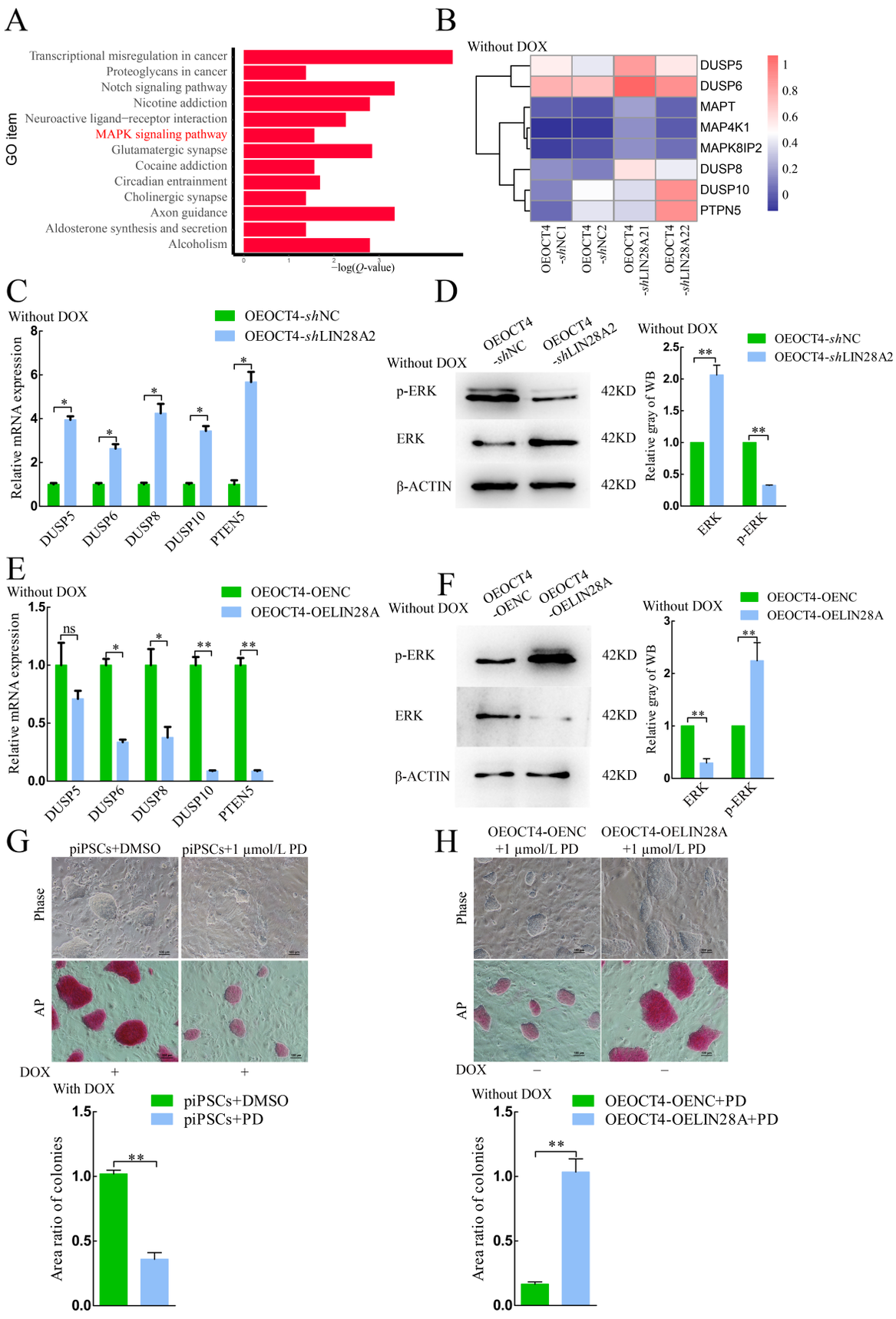
A
Transcriptional misregulation in cancer
Proteoglycans in cancer
Notch signaling pathway
Nicotine addiction
Neuroactive ligand−receptor interaction
MAPK signaling pathway
Glutamatergic synapse
Cocaine addiction
Circadian entrainment
Cholinergic synapse
Axon guidance
Aldosterone synthesis and secretion
Alcoholism
GO item
−log(Q-value)
B
Without DOX
DUSP5
DUSP6
MAPT
MAP4K1
MAPK8IP2
DUSP8
DUSP10
PTPN5
OEOCT4 -shNC1
OEOCT4 -shNC2
OEOCT4 -shLIN28A21
OEOCT4 -shLIN28A22
C
Without DOX
OEOCT4-shNC
OEOCT4-shLIN28A2
Relative mRNA expression
DUSP5
DUSP6
DUSP8
DUSP10
PTEN5
D
Without DOX
OEOCT4 -shNC
OEOCT4 -shLIN28A2
p-ERK
ERK
β-ACTIN
42KD
Relative gray of WB
E
Without DOX
OEOCT4-OENC
OEOCT4-OELIN28A
Relative mRNA expression
ns
F
Without DOX
OEOCT4 -OENC
OEOCT4 -OELIN28A
p-ERK
ERK
β-ACTIN
42KD
Relative gray of WB
G
piPSCs+DMSO
piPSCs+1 μmol/L PD
Phase
AP
DOX
With DOX
piPSCs+DMSO
piPSCs+PD
Area ratio of colonies
H
OEOCT4-OENC +1 μmol/L PD
OEOCT4-OELIN28A +1 μmol/L PD
Phase
AP
DOX
Without DOX
OEOCT4-OENC+PD
OEOCT4-OELIN28A+PD
Area ratio of colonies

Figure 4 *LIN28A* inhibited *DUSP*-family expression and activated MAPK signaling pathway

A: KEGG enrichment analysis of up-regulated DEGs, highlighting the MAPK signaling pathway. B: Heat map showing mRNA expression of *DUSP* family in OEOCT4-*sh*NC and OEOCT4-*sh*LIN28A2 groups without DOX based on RNA-seq. C: mRNA expression levels of *DUSP* family in OEOCT4-*sh*NC and OEOCT4-*sh*LIN28A2 groups without DOX were detected by qRT-PCR. Data are mean±*SEM*. *: P<0.05. n=3. D: Left: Protein expression levels of ERK/p-ERK in OEOCT4-*sh*NC and OEOCT4-*sh*LIN28A2 groups without DOX were detected by western blotting. Right: Quantitative analysis is shown in histogram. Data are mean±*SEM*. **: P<0.01. n=2. E: Left: mRNA expression levels of *DUSP* family in OEOCT4-OENC and OEOCT4-OELIN28A groups without DOX were detected by qRT-PCR. Data are mean±*SEM*. *: P<0.05, **: P<0.01. n=3. F: Left: ERK/p-ERK protein expression levels in OEOCT4-OENC and OEOCT4-OELIN28A groups without DOX were detected by western blotting. Right: Quantitative analysis is shown in histogram. Data are mean±*SEM*. **: P<0.01. n=2. G: Up: Morphology and AP staining of piPSCs with addition of DMSO and 1.0 μmol/L PD0325901 with DOX. Scale bar: 100 μm. Down: Area ratio of colonies in piPSCs with addition of DMSO and 1.0 μmol/L PD0325901 with DOX. **: P<0.01. H: Up: Morphology and AP staining of OEOCT4-OENC and OEOCT4-OELIN28A groups with addition of 1.0 μmol/L PD0325901 without DOX. Down: Area ratio of colonies in OEOCT4-OENC and OEOCT4-OELIN28A groups with addition of 1.0 μmol/L PD0325901 without DOX. **: P<0.01.

LIN28B showed no significant changes, indicating that knockdown of *LIN28A* did not affect *LIN28B* expression. *LIN28A* also plays an important role in nervous system development (Faunes, 2020; Romer-Seibert et al., 2019; Yermalovich et al., 2020). The expression of genes involved in the negative regulation of cell proliferation, neuronal differentiation, and positive regulation of cell differentiation also increased in the OEOCT4-*sh*LIN28A2 group (Figure 3D–F). Thus, after *LIN28A* knockdown, the pluripotency of piPSCs disappeared, the proliferation ability of piPSCs decreased, and the piPSCs differentiated into neuroectoderm cells. These results are consistent with previous study, which found that miR-370 can inhibit the expression of *LIN28A* (Zhang et al., 2017). To further explore its function, porcine *LIN28A* was overexpressed in the piPSCs. However, colony size, proliferation ability, and AP activity demonstrated no significant change after *LIN28A* overexpression. This was not obvious with the addition of DOX but was observed after the withdrawal of DOX. The OELIN28A+DOX− group maintained typical colonies, whereas the OENC+DOX− group did not (Figure 1E), suggesting that *LIN28A* plays an important role in maintaining the proliferation ability of piPSCs.

Previous immunohistochemical analysis reported that ERK phosphorylation is up-regulated in *Lin28a* transgenic mice (Kobayashi & Kozlova, 2018), which, in turn, promotes the phosphorylation and protein stability of LIN28A (Tsanov & Daley, 2017; Tsanov et al., 2017). We found that *LIN28A* inhibited the expression of *DUSP*-family phosphatases, which activated ERK signaling (Figure 4C–F). The mRNA expression levels of *DUSP6/8/10* were markedly up-regulated after *LIN28A* knockdown. As a member of the *DUSP* family, *DUSP6/8/10* inhibits ERK activity to regulate MAPK signaling in ovarian epithelial cancer (Gao et al., 2020), pancreatic cancer (Liu et al., 2021), and human epidermal stem cells (Hiratsuka et al., 2020). The increase in *DUSP6/8/10* expression indicates inactivation of MAPK signaling (Cornacchia et al., 2019). The weakly positive AP activity in the *sh*LIN28A1/2 and OEOCT-*sh*LIN28A2 groups was consistent with the results obtained when DOX-piPSCs were supplemented 1.0 μmol/L MEK1 inhibitor PD0325901 (Figures 1C, 2F, 4G). *In vitro*, MAPK is the key for maintaining the primed state, whereas PSCs transform into the naïve state with MAPK signaling repression (Chen et al., 2015; Hackett & Surani, 2014; Ying et al., 2008). However, the pluripotency of piPSCs is rapidly lost with 1.0 μmol/L MEK1 inhibitor PD0325901 (Gao et al., 2019). This indicated that inactivation of MAPK signaling impaired the pluripotency of piPSCs. We demonstrated that *LIN28A* maintained the pluripotency piPSCs by activating the MAPK signaling pathway. Therefore, further investigations on the molecular mechanisms underlying how *LIN28A* regulates its downstream genes and interacts with other transcription factors in piPSCs are warranted.

SUPPLEMENTARY DATA

Supplementary data to this article can be found online.

COMPETING INTERESTS

The authors declare that they have no competing interests.

AUTHOR CONTRIBUTIONS

X.L.W., Z.S.Z., and J.L.H. designed the research. X.L.W., Z.S.Z., Z.Z., and S.Y. performed the research. X.L.W., X.X, and J.L.H. wrote the paper. X.X, Q.Y.S., and M.Z.L analyzed the data. X.L.W., Z.S.Z., J.Q.Z, W.Y., R.Z., X.H., S.P., S.Q.Z., N.L., M.Z.L, and J.L.H. modified the manuscript. All authors read and approved the final version of the manuscript.

ACKNOWLEDGMENTS

The authors thank Dr. Ying Zhang and Fang-Lin Ma for helpful comments on this paper.

REFERENCES

Balzer E, Heine C, Jiang Q, Lee VM, Moss EG. 2010. LIN28 alters cell fate succession and acts independently of the *let-7* microRNA during neurogliogenesis in vitro. *Development*, **137**(6): 891−900.

Buganim Y, Faddah DA, Cheng AW, Itskovich E, Markoulaki S, Ganz K, et al. 2012. Single-cell expression analyses during cellular reprogramming reveal an early stochastic and a late hierarchic phase. *Cell*, **150**(6): 1209−1222.

Burdon T, Stracey C, Chambers I, Nichols J, Smith A. 1999. Suppression of SHP-2 and ERK signalling promotes self-renewal of mouse embryonic stem cells. *Developmental Biology*, **210**(1): 30−43.

Caunt CJ, Keyse SM. 2013. Dual-specificity MAP kinase phosphatases (MKPs): shaping the outcome of MAP kinase signalling. *FEBS Journal*,

280(2): 489−504.

Chandrasekaran S, Zhang J, Sun Z, Zhang L, Ross CA, Huang YC, et al. 2017. Comprehensive mapping of pluripotent stem cell metabolism using dynamic genome-scale network modeling. *Cell Reports*, **21**(10): 2965−2977.

Chen HF, Chuang HC, Tan TH. 2019. Regulation of dual-specificity phosphatase (DUSP) ubiquitination and protein stability. *International Journal of Molecular Sciences*, **20**(11): 2668.

Chen HX, Guo RP, Zhang Q, Guo HC, Yang M, Wu ZF, et al. 2015. Erk signaling is indispensable for genomic stability and self-renewal of mouse embryonic stem cells. *Proceedings of the National Academy of Sciences of the United States of America*, **112**(44): E5936−E5943.

Cheng D, Guo YJ, Li ZZ, Liu YJ, Gao X, Gao Y, et al. 2012. Porcine induced pluripotent stem cells require LIF and maintain their developmental potential in early stage of embryos. *PLoS One*, **7**(12): e51778.

Chomczynski P, Sacchi N. 2006. The single-step method of RNA isolation by acid guanidinium thiocyanate-phenol-chloroform extraction: twenty-something years on. *Nature Protocols*, **1**(2): 581−585.

Cornacchia D, Zhang C, Zimmer B, Chung SY, Fan YJ, Soliman MA, et al. 2019. Lipid deprivation induces a stable, naive-to-primed intermediate state of pluripotency in human PSCs. *Cell Stem Cell*, **25**(1): 120−136.

Deathridge J, Antolović V, Parsons M, Chubb JR. 2019. Live imaging of ERK signalling dynamics in differentiating mouse embryonic stem cells. *Development*, **146**(12): dev172940.

Esteban MA, Xu JY, Yang JY, Peng MX, Qin DJ, Li W, et al. 2009. Generation of induced pluripotent stem cell lines from tibetan miniature pig. *Journal of Biological Chemistry*, **284**(26): 17634−17640.

Ezashi T, Telugu BPVL, Alexenko AP, Sachdev S, Sinha S, Roberts RM. 2009. Derivation of induced pluripotent stem cells from pig somatic cells. *Proceedings of the National Academy of Sciences of the United States of America*, **106**(27): 10993−10998.

Faunes F. 2020. Role and Regulation of Lin28 in Progenitor Cells During Central Nervous System Development. New York: Springer.

Gao XF, Nowak-Imialek M, Chen X, Chen DS, Herrmann D, Ruan DG, et al. 2019. Establishment of porcine and human expanded potential stem cells. *Nature Cell Biology*, **21**(6): 687−699.

Gao Y, Li H, Han Q, Li Y, Wang TX, Huang CY, et al. 2020. Overexpression of DUSP6 enhances chemotherapy-resistance of ovarian epithelial cancer by regulating the ERK signaling pathway. *Journal of Cancer*, **11**(11): 3151−3164.

Hackett JA, Surani MA. 2014. Regulatory principles of pluripotency: from the ground state up. *Cell Stem Cell*, **15**(4): 416−430.

Hafner M, Max KEA, Bandaru P, Morozov P, Gerstberger S, Brown M, et al. 2013. Identification of mRNAs bound and regulated by human LIN28 proteins and molecular requirements for RNA recognition. *RNA*, **19**(5): 613−626.

Haraguchi S, Kikuchi K, Nakai M, Tokunaga T. 2012. Establishment of self-renewing porcine embryonic stem cell-like cells by signal inhibition. *Journal of Reproduction and Development*, **58**(6): 707−716.

Hiratsuka T, Bordeu I, Pruessner G, Watt FM. 2020. Regulation of ERK basal and pulsatile activity control proliferation and exit from the stem cell compartment in mammalian epidermis. *Proceedings of the National Academy of Sciences of the United States of America*, **117**(30): 17796−17807.

Hou DR, Jin Y, Nie XW, Zhang ML, Ta N, Zhao LH, et al. 2016. Derivation of porcine embryonic stem-like cells from *in vitro*-produced blastocyst-stage embryos. *Scientific Reports*, **6**: 25838.

Hu X, Wang M, Cao L, Cong L, Gao YJ, Lu JW, et al. 2020. MiR-4319 suppresses the growth of esophageal squamous cell carcinoma via targeting NLRC5. *Current Molecular Pharmacology*, **13**(2): 144−149.

Kalkan T, Bornelov S, Mulas C, Diamanti E, Lohoff T, Ralser M, et al. 2019. Complementary activity of ETV5, RBPJ, and TCF3 drives formative transition from naive pluripotency. *Cell Stem Cell*, **24**(5): 785−801.

Kobayashi T, Kozlova A. 2018. Lin28a overexpression reveals the role of Erk signaling in articular cartilage development. *Development*, **145**(15): dev162594.

Kumar RM, Cahan P, Shalek AK, Satija R, Daleykeyser AJ, Li H, et al. 2014. Deconstructing transcriptional heterogeneity in pluripotent stem cells. *Nature*, **516**(7529): 56−61.

Liao J, Wu Z, Wang Y, Cheng L, Cui C, Gao Y, et al. 2008. Enhanced efficiency of generating induced pluripotent stem (iPS) cells from human somatic cells by a combination of six transcription factors. *Cell Research*, **18**(5): 600−603.

Liu MQ, Qin Y, Hu QS, Liu WS, Ji SR, Xu WY, et al. 2021. SETD8 potentiates constitutive ERK1/2 activation via epigenetically silencing DUSP10 expression in pancreatic cancer. *Cancer Letters*, **499**: 265−278.

Ma FL, Du XM, Wei YD, Zhou Z, Clotaire DZJ, Li N, et al. 2019. *LIN28A* activates the transcription of *NANOG* in dairy goat male germline stem cells. *Journal of Cellular Physiology*, **234**(6): 8113−8121.

Ma YY, Yu T, Cai YX, Wang HY. 2018. Preserving self-renewal of porcine pluripotent stem cells in serum-free 3i culture condition and independent of LIF and b-FGF cytokines. *Cell Death Discovery*, **4**: 21.

Marks H, Kalkan T, Menafra R, Denissov S, Jones K, Hofemeister H, et al. 2012. The transcriptional and epigenomic foundations of ground state pluripotency. *Cell*, **149**(3): 590−604.

Moss EG, Lee RC, Ambros V. 1997. The cold shock domain protein LIN-28 controls developmental timing in C. elegans and is regulated by the *lin-4* RNA. *Cell*, **88**(5): 637−646.

Pearson G, Robinson F, Beers Gibson T, Xu BE, Karandikar M, Berman K, et al. 2001. Mitogen-activated protein (MAP) kinase pathways: regulation and physiological functions. *Endocrine Reviews*, **22**(2): 153−183.

Polesskaya A, Cuvellier S, Naguibneva I, Duquet A, Moss EG, Harel-Bellan A. 2007. Lin-28 binds IGF-2 mRNA and participates in skeletal myogenesis by increasing translation efficiency. *Genes & Development*, **21**(9): 1125−1138.

Richards M, Tan SP, Tan JH, Chan WK, Bongso A. 2004. The transcriptome profile of human embryonic stem cells as defined by SAGE. *Stem Cells*, **22**(1): 51−64.

Romer-Seibert JS, Hartman NW, Moss EG. 2019. The RNA-binding protein LIN28 controls progenitor and neuronal cell fate during postnatal neurogenesis. *FASEB Journal*, **33**(3): 3291−3303.

Sang H, Wang D, Zhao S, Zhang JX, Zhang Y, Xu J, et al. 2019. Dppa3 is critical for Lin28a-regulated ES cells naïve-primed state conversion. *Journal of Molecular Cell Biology*, **11**(6): 474−488.

Shaul YD, Seger R. 2007. The MEK/ERK cascade: from signaling specificity to diverse functions. *Biochimica Et Biophysica Acta (BBA)-Molecular Cell Research*, **1773**(8): 1213−1226.

Shyh-Chang N, Daley GQ. 2013. Lin28: primal regulator of growth and metabolism in stem cells. *Cell Stem Cell*, **12**(4): 395−406.

Tsanov KM, Daley GQ. 2017. Signaling through RNA-binding proteins as a

cell fate regulatory mechanism. *Cell Cycle*, **16**(8): 723−724.

Tsanov KM, Pearson DS, Wu ZT, Han A, Triboulet R, Seligson MT, et al. 2017. LIN28 phosphorylation by MAPK/ERK couples signalling to the post-transcriptional control of pluripotency. *Nature Cell Biology*, **19**(1): 60−67.

Wei YD, Du XM, Yang DH, Ma FL, Yu XW, Zhang MF, et al. 2021. Dmrt1 regulates the immune response by repressing the TLR4 signaling pathway in goat male germline stem cells. *Zoological Research*, **42**(1): 14−27.

Xu BS, Zhang KX, Huang YQ. 2009. Lin28 modulates cell growth and associates with a subset of cell cycle regulator mRNAs in mouse embryonic stem cells. *RNA*, **15**(3): 357−361.

Xu JJ, Zheng Z, Du XG, Shi BB, Wang JC, Gao DF, et al. 2020. A cytokine screen using CRISPR-Cas9 knock-in reporter pig iPS cells reveals that Activin A regulates *NANOG*. *Stem Cell Research & Therapy*, **11**(1): 67.

Xue BH, Li Y, He YL, Wei RY, Sun RZ, Yin Z, et al. 2016. Porcine pluripotent stem cells derived from IVF embryos contribute to chimeric development *in vivo*. *PLoS One*, **11**(3): e0151737.

Yang DH, Moss EG. 2003. Temporally regulated expression of Lin-28 in diverse tissues of the developing mouse. *Gene Expression Patterns*, **3**(6): 719−726.

Yermalovich AV, Osborne JK, Sousa P, Han A, Kinney MA, Chen MJ, et al. 2020. Author correction: Lin28 and *let-7* regulate the timing of cessation of murine nephrogenesis. *Nature Communications*, **11**(1): 1327.

Ying QL, Wray J, Nichols J, Batlle-Morera L, Doble B, Woodgett J, et al. 2008. The ground state of embryonic stem cell self-renewal. *Nature*, **453**(7194): 519−523.

Yu JY, Vodyanik MA, Smuga-Otto K, Antosiewicz-Bourget J, Frane JL, Tian SL, et al. 2007. Induced pluripotent stem cell lines derived from human somatic cells. *Science*, **318**(5858): 1917−1920.

Zhang J, Ratanasirintrawoot S, Chandrasekaran S, Wu ZT, Ficarro SB, Yu CX, et al. 2016. LIN28 regulates stem cell metabolism and conversion to primed pluripotency. *Cell Stem Cell*, **19**(1): 66−80.

Zhang SQ, Guo YJ, Cui Y, Liu YJ, Yu T, Wang HY. 2015. Generation of intermediate porcine iPS cells under culture condition favorable for mesenchymal-to-epithelial transition. *Stem Cell Reviews and Reports*, **11**(1): 24−38.

Zhang SQ, Xie YL, Cao HX, Wang HY. 2017. Common microRNA-mRNA interactions exist among distinct porcine iPSC lines independent of their metastable pluripotent states. *Cell Death & Disease*, **8**(8): e3027.

Zhu H, Shyh-Chang N, Segrè AV, Shinoda G, Shah SP, Einhorn WS, et al. 2011. The *Lin28/let-7* axis regulates glucose metabolism. *Cell*, **147**(1): 81−94.

Zhu ZS, Pan Q, Zhao WX, Wu XL, Yu S, Shen QY, et al. 2021. BCL2 enhances survival of porcine pluripotent stem cells through promoting FGFR2. *Cell Proliferation*, **54**(1): e12932.

Zhu ZS, Wu XL, Li Q, Zhang JQ, Yu S, Shen QY, et al. 2021. Histone demethylase complexes KDM3A and KDM3B cooperate with OCT4/SOX2 to define a pluripotency gene regulatory network. *FASEB Journal*, doi: 10.1096/fj.202100230R.